

# Ultrasonic-Assisted Synthesis of Au Nanobelts and Nanowires

Yingzhou Huang<sup>1</sup>, Wenzhong Wang<sup>2,\*</sup>, Hongyan Liang<sup>1,3</sup>, Hong Wei<sup>1</sup>, and Hongxing Xu<sup>1,\*</sup>

<sup>1</sup>*Institute of Physics, Chinese Academy of Sciences, Beijing 100190, China*

<sup>2</sup>*School of Science, Minzu University of China, Beijing 100081, China*

<sup>3</sup>*School of Materials Science and Engineering, Shandong University, Jinan 250100, China*

Au one-dimensional (1D) nanostructures, including nanobelts and nanowires, have been synthesized in an ethylene glycol (EG)/polyvinylpyrrolidone (PVP) system by a simple and convenient seed-mediated growth method. The nanobelts and nanowires have aspect ratios up to 600, a length distribution ranging from several to tens of microns, and an average width of 100 nm. In this method, we used an ultrasonic process to promote the formation of Au seeds, which largely determines the morphology of final product. Additionally, we have found that the ultrasonic process significantly increases the fabrication yield of 1D nanostructures. Further experimental results show strong polarization dependence of Surface-Enhanced Raman Scattering (SERS) on a single Au 1D nanostructure. This convenient, versatile and low-cost synthesis method can be applied to 1D nanostructures composed from a range of materials, making it widely applicable to many areas of modern science and technology.

**Keywords:** Ultrasonic, Synthesis, Au Nanobelts, Au Nanowires, SERS.

## 1. INTRODUCTION

Au and Ag nanostructures attracted a great deal of interest largely due to their intense plasmon absorption bands in the ultraviolet, visible, and near-infrared wavelength regime, which can be modified by varying their size and shape. These properties make Au and Ag nanostructures extremely useful in a variety of spectroscopic applications, such as SERS, surface-enhanced fluorescence (SEF), two-photon luminescence, optical force and surface plasmon resonance (SPR) spectroscopy.<sup>1–11</sup> Compared to other nanostructures, 1D nanostructures in form of nanorods, nanowires, nanotubes or nanobelts are the ideal materials to investigate the dependence of electrical and thermal transport as well as optical and mechanical properties on dimensionality and size reduction.<sup>12–15</sup>

Various methods of synthesis of Au and Ag 1D nanostructures have been reported in the literature, including chemical vapor deposition, photochemical, electroless and electrochemical deposition and wet chemical methods involving templates, surfactants, and capping agents.<sup>16–22</sup> Seed-mediated growth methods for the fabrication of Au nanostructures have been adopted extensively due to their high yield, speed of synthesis and ease of control.<sup>21–22</sup> Sonochemical synthesis, which has received much attention recently,<sup>23–30</sup> is another powerful method used to

generate various types of nanostructures composed of noble metals, transition metals, semiconductors, carbon materials, and polymeric materials. The advantages of this method include a rapid reaction rate compared with chemical synthesis and the ability to form very small nanoparticles, which could be used as seeds in the seed-mediated growth synthesis. Therefore we explore a new strategy regarding the preparation of colloidal Au 1D nanostructures by a seed-mediated growth method assisted by ultrasound.

## 2. EXPERIMENTAL DETAILS

HAuCl<sub>4</sub> · 4H<sub>2</sub>O, NaBH<sub>4</sub>, PVP (K30, Mw = 30 000) and EG were provided by the Beijing Analytical Instrument Factory. Deionized water was used in all processes. To synthesize Au nanobelts and nanowires, 444 mg PVP was dissolved into a 40 ml solution of EG using continuous magnetic stirring. Next, a NaBH<sub>4</sub> solution (0.01 mL, 0.2 M) was introduced under stirring. After 1–2 min, an aqueous HAuCl<sub>4</sub> solution (0.3 mL, 0.5 M) was added. These operations were performed at room temperature. Then the solution was transferred into a Teflon vessel with 100 ml capacity and appeared yellow due to the presence of Au<sup>3+</sup> ions. The solution was then subjected to high-intensity ultrasound irradiation (40 kHz, 100 W) at 50 °C for 6 hours and, afterwards, sealed in

\*Authors to whom correspondence should be addressed.

a stainless-steel bomb. The entire system was then heated and maintained at 160 °C under auto-generated pressure for 12 hours. Once the reaction was completed, the container was allowed to cool to ambient temperature and the products were collected by centrifugation (6000 rpm).

SERS spectra of Malachite green isothiocyanate (MGITC) on single Au nanobelts and nanowires was excited by a 632.8 nm He–Ne laser. To get a SERS sample, first a MGITC ethanol solution (0.065 mM) mixed with product was spin-coated on the Si substrate. Then a marked TEM grid was taped to the substrate. This could help us obtain scanning electron microscopy (SEM) image and SERS spectrum at the same position. And the polarization of the laser was varied using a half wave plate.

### 3. RESULTS AND DISCUSSION

As shown in Figure 1(A), the FESEM images show several high aspect ratio 1D nanostructures mixed with nanoparticles in the as-prepared product. To further analyze the characteristics of these 1D nanostructures, high-magnification SEM (HMSEM) images were taken (Figs. 1(B and C)). In these images, it is clear that these nanostructures are indeed nanobelts and nanowires with widths of about 100 nm. X-ray diffraction (XRD) pattern indicates that the five diffraction peaks shown in Figure 2(A) correspond to the (111), (200), (220), (311) and (222) diffraction peaks of Au, indicating that the product is composed of pure crystalline Au. These observations confirm that the as-prepared nanostructures are primarily dominated by (111) facets and thus their (111) planes tend to be preferentially oriented parallel to the surface of the supporting substrate. The composition of the product has been analyzed by an energy-dispersive X-ray (EDX) spectrometer equipped with SEM. The signal collected over the sample shown in Figure 2(B) gives further support to the notion that the product consists only of Au. To further elucidate the structure of the Au nanobelts and nanowires in detail, transmission electron microscopy (TEM) images are shown in Figures 3(A and E). It can be seen from high-magnification TEM images in Figures 3(B and F) that both the Au nanobelts and nanowires have smooth

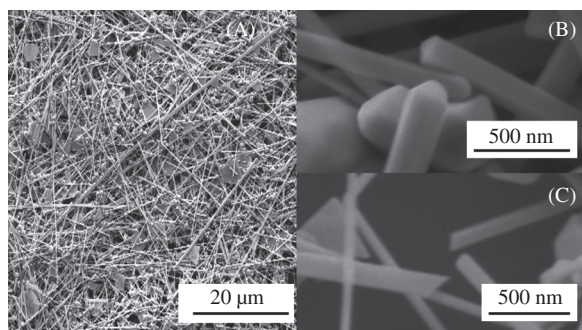


**Fig. 1.** (A) Low- and (B), (C) high-magnification SEM images of the as-prepared Au 1D nanostructures.

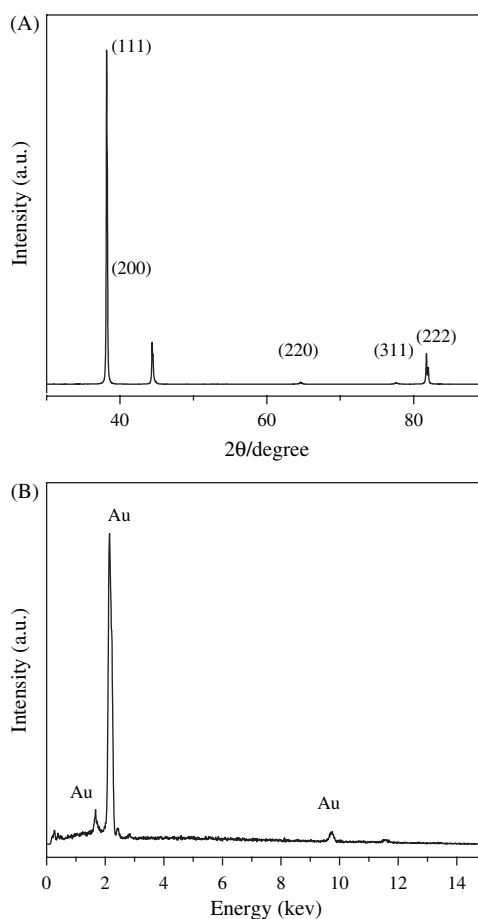


**Fig. 2.** A) XRD patterns and (B) EDX spectrometry data of the as-prepared Au 1D.

sides. Furthermore, the thickness of nanobelts is approximate 20 nm. Selected area electron diffraction (SAED) patterns and high-resolution TEM (HRTEM) images in Figures 3(C, G, D and H) demonstrate that the nanobelts are single crystals with stacking faults and the nanowires are five fold twinned crystals.

Further experiments revealed that the introduction of both the reducing reagent  $\text{NaBH}_4$  and the ultrasonic process were two key parameters in increasing the relative yield of Au 1D nanostructures. When the  $\text{NaBH}_4$  was not added to the precursor solution (Fig. 4(A)) or the precursor solution was not kept in the ultrasonic bath but instead heated directly to the reaction temperature at 160 °C (Fig. 4(B)), or both the reducing reagent  $\text{NaBH}_4$  and the ultrasonic process were not taken into the synthesis (Fig. 4(C)), the majority (>90%) of the final product was nanoparticles with various shapes. In our experiment the color of the solution remained pale yellow (the color of Au salts) after the addition of  $\text{NaBH}_4$ , indicating that the concentration of  $\text{NaBH}_4$  was less than stoichiometric. Specifically, this means that only some of the  $\text{Au}^{3+}$  ions were reduced to  $\text{Au}^0$  atoms, making them available for oxidation by the remaining  $\text{Au}^{3+}$ . This caused the number

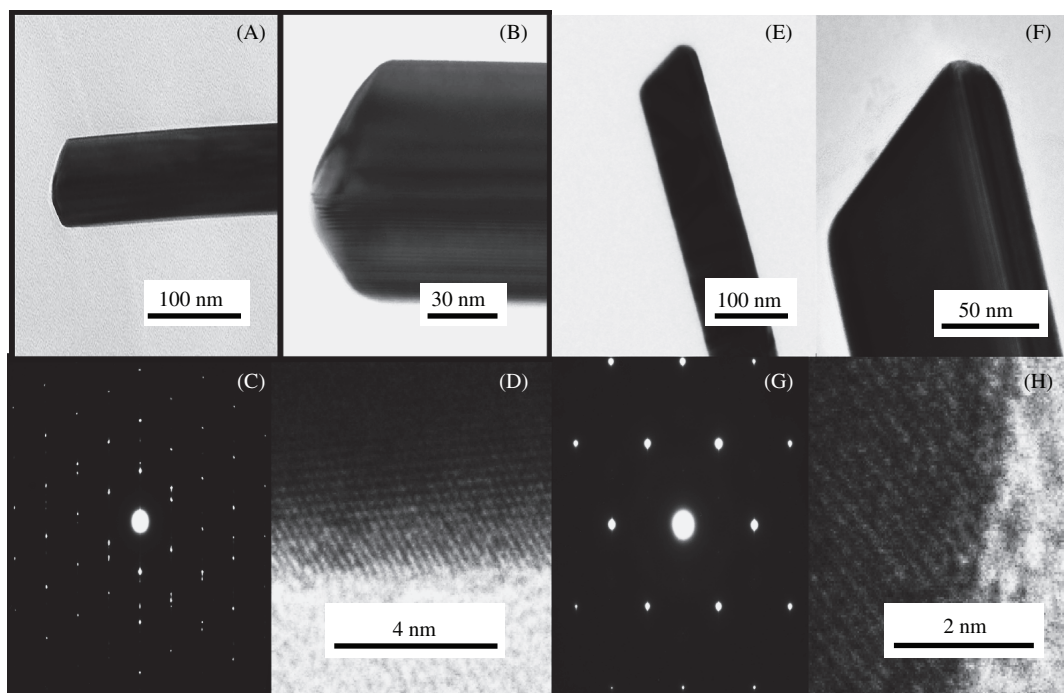


**Fig. 3.** (A) Low- and (B) high-magnification TEM images (C) SAED patterns (D) HRTEM image of the as-prepared Au nanowires. (E) Low- and (F) high-magnification TEM images (G) SAED patterns (H) HRTEM image of the as-prepared Au nanobelts.

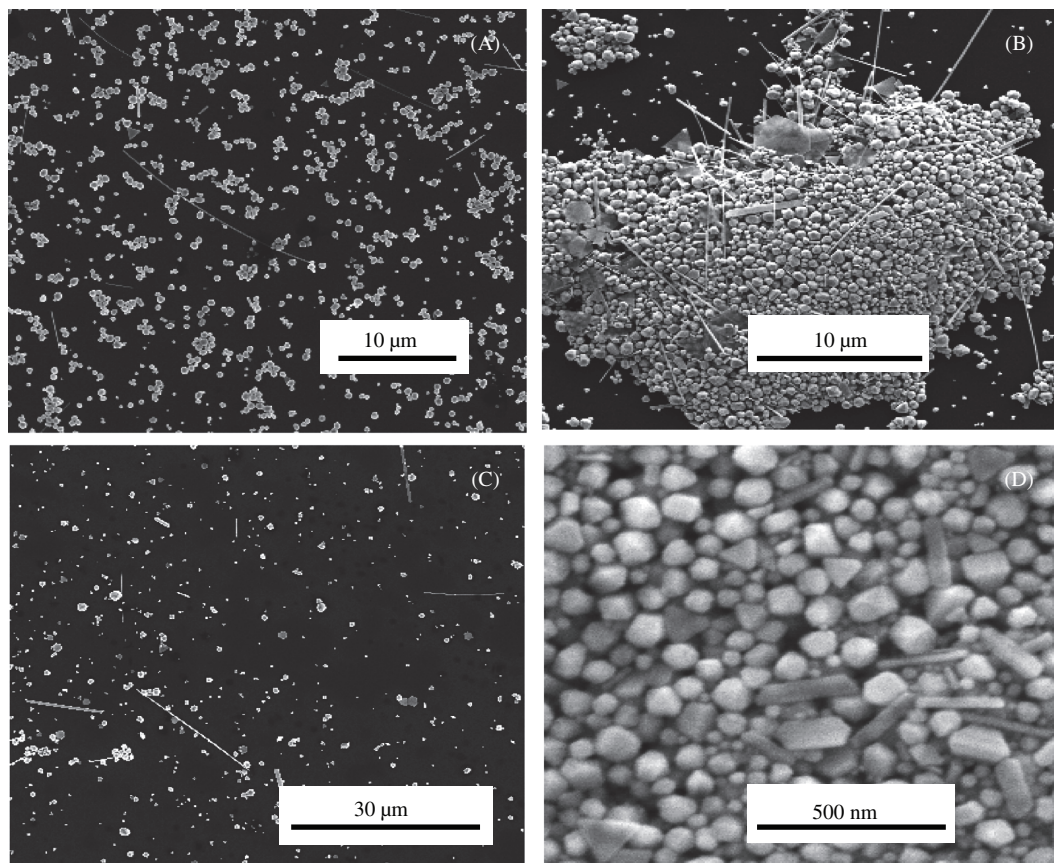


**Fig. 4.** (A) sample without  $\text{NaBH}_4$  (B) sample without ultrasonic process (C) sample without both  $\text{NaBH}_4$  and ultrasonic process (D) seeds produced by both  $\text{NaBH}_4$  and ultrasonic process.

RESEARCH ARTICLE

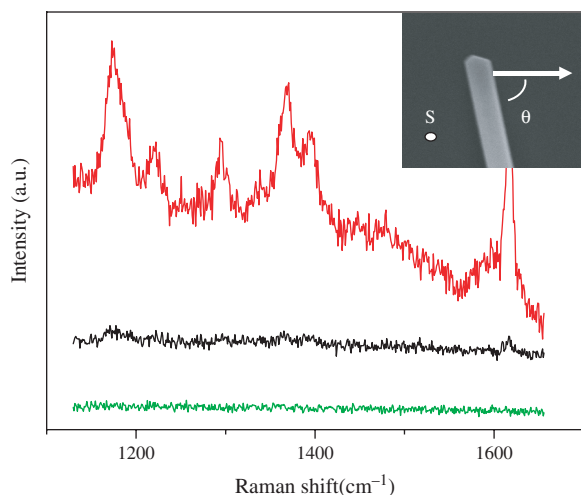


**Fig. 5.** SERS spectra of MGITC adsorbed on a single Au 1D nanostructure. The spectrum obtained for  $\theta = 90^\circ$  (red),  $\theta = 0^\circ$  (black) and at point  $S$  (green), respectively. Inset is SEM image of a single Au 1D nanostructure.

of the  $\text{Au}^+$  ions in the solution to increase in comparison to the solution without  $\text{NaBH}_4$ . During the ultrasonic process, the color of the solution changed to light brown, indicating that Au seeds had been formed (Fig. 4(D)). The extreme conditions of transient high temperature and high pressure provided by acoustic cavitations cause the EG and PVP to decompose into radicals (particularly, the hydroxyl radical) which reduces Au salts into Au nanostructures. Additionally, the temperature increase resulting from the ultrasonically generated heat may partly contribute the formation of the Au seeds. After the ultrasonic process, the reaction temperature was increased to above  $160^\circ\text{C}$ , the Au ions were reduced to Au atoms by the so-called polyol process, resulting in the synthesis of Au nanostructures.

Figure 5 shows the polarization dependence of the SERS spectra of MGITC adsorbed on a single Au 1D nanostructure.  $S$  is a spot where the laser is focused outside the Au 1D nanostructure to obtain a SERS spectrum of MGITC on the Si substrate for comparison.  $\theta$  is the angle between the Au 1D nanostructure and the polarization of light. Spectra were obtained for  $\theta = 90^\circ$ ,  $\theta = 0^\circ$  and at point  $S$ , respectively. These measurements demonstrate that the SERS signal was strongly enhanced when  $\theta = 90^\circ$  compared to  $\theta = 0^\circ$  and at the  $S$  point, indicating that the strongly anisotropic SERS signal could be induced by the localized excitation of a single Au 1D nanostructure.

#### 4. CONCLUSIONS

In summary, we have developed an ultrasonic assisted method of synthesis for Au nanobelts and nanowires with

high aspect ratios. The fabrication of Au 1D nanostructures by an ultrasonic process has been discussed experimentally. Also we have demonstrated the strong polarization dependence of SERS on a single Au 1D nanostructure. This novel method will improve the application of 1D nanostructure on modern science and technology.

#### References and Notes

1. S. Nie and S. R. Emory, *Science* 275, 1102 (1997).
2. K. Kneipp, Y. Wang, H. Kneipp, L. T. Perelman, I. Itzkan, R. R. Dasari, and M. S. Feld, *Phys. Rev. Lett.* 78, 1667 (1997).
3. H. X. Xu, E. J. Bjerneld, M. Kall, and L. Borjesson, *Phys. Rev. Lett.* 83, 4357 (1999).
4. M. T. Sun, S. B. Wan, Y. J. LIU, Y. Jia, and H. X. Xu, *J. Raman Spectrosc.* 39, 402 (2008).
5. A. Parfenov, I. Gryczynski, J. Malicka, C. D. Geddes, and J. R. Lakowicz, *J. Phys. Chem. B* 107, 8829 (2003).
6. A. Ashkin, J. M. Dziedzic, J. E. Bjorkholm, and S. Chu, *S. Opt. Lett.* 11, 288 (1986).
7. H. Wang, T. B. Huff, D. A. Zweifel, W. He, P. S. Low, A. Wei, and J. Cheng, *Proc. Natl. Acad. Sci. USA* 102, 15752 (2005).
8. Z. P. Li, H. X. Xu, and M. Kall, *Phys. Rev. B* 77, 085412 (2008).
9. F. Svedberg, Z. P. Li, H. X. Xu, and M. Kall, *Nano Lett.* 6, 2639 (2006).
10. L. A. Lyon, M. D. Musick, and M. J. Natan, *Anal. Chem.* 70, 5177 (1998).
11. Z. L. Wang, R. P. Gao, Z. W. Pan, and Z. R. Dai, *Adv. Eng. Mater.* 3, 657 (2001).
12. Y. N. Xia, P. D. Yang, Y. G. Sun, Y. Y. Wu, B. Mayers, B. Gates, Y. D. Yin, F. Kim, and H. O. Yan, *Adv. Mater.* 15, 353 (2003).
13. Z. L. Wang, *Adv. Mater.* 15, 432 (2003).
14. G. A. Baker, *Adv. Mater.* 17, 639 (2003).
15. M. Tian, J. Wang, J. Kurtz, T. E. Mallouk, and M. H. W. Chan, *Nano Lett.* 3, 919 (2003).
16. M. Wirtz and C. R. Martin, *Adv. Mater.* 15, 455 (2003).
17. P. Forrer, F. Schlottig, H. Siegenthaler, and M. J. Textor, *Appl. Electrochem.* 30, 533 (2000).
18. C. R. Martin, *Science* 266, 1961 (1993).
19. Y. G. Sun, B. Gates, B. Mayers, and Y. N. Xia, *Nano Lett.* 2, 165 (2002).
20. N. R. Jana, L. Gearheart, and C. J. Murphy, *J. Phys. Chem. B* 105, 4065 (2001).
21. T. K. Sau and C. J. Murphy, *J. Am. Chem. Soc.* 126, 8648 (2004).
22. K. S. Suslick and G. J. Price, *Annu. Rev. Mater. Sci.* 29, 295 (1999).
23. K. S. Suslick, S. B. Choe, A. A. Cichowlas, and M. W. Grinstaff, *Nature* 353, 414 (1991).
24. N. A. Dhas and A. J. Gedanken, *Phys. Chem. B* 101, 9495 (1997).
25. S. Ramesh, Y. Kolytyn, R. Prozorov, and A. Gedanken, *Chem. Mater.* 9, 546 (1997).
26. R. A. Hobson, P. Mulvaney, and F. Grieser, *J. Chem. Soc., Chem. Commun.* 7, 823 (1994).
27. R. Katoh, Y. Tasaka, E. Sekreta, M. Yumura, F. Ikazaki, Y. Kakudate, and S. Fujiwara, *Ultrasonics Sonochem.* 6, 185 (1999).
28. M. Bradley, M. Ashokkumar, and F. Grieser, *J. Am. Chem. Soc.* 125, 525 (2003).
29. K. Okitsu, Y. Mizukoshi, H. Bandow, A. T. Yamamoto, Y. Nagata, and Y. Maeda, *J. Phys. Chem. B* 101, 5470 (1997).
30. Z. L. Wang, *J. Phys. Chem. B* 104, 1153 (2000).

Received: 4 September 2009. Accepted: 30 October 2009.